Supplement of Biogeosciences, 20, 2347–2367, 2023
https://doi.org/10.5194/bg-20-2347-2023-supplement

Biogeosciences Open Access EGU

Supplement of

Biogeochemical processes captured by carbon isotopes in redox-stratified water columns: a comparative study of four modern stratified lakes along an alkalinity gradient

Robin Havas et al.

Correspondence to: Robin Havas (robin.havas@gmail.com)

Supplementary Text

I. Offset between O_2 exhaustion and ORP decrease

In lakes Alberca and Alchichica, there is a large offset between the depth where O_2 reaches ~0 and that where the oxidation reduction potential (ORP) starts to decrease (~7 and 10m differences, respectively). In lakes La Preciosa and Atexcac, this difference is less important (< 2m). Two possibilities could explain this discrepancy. First, we notice that the ORP usually starts decreasing after a turbidity peak appeared, likely corresponding to Mn-oxides precipitation (cf. Fig. 2). It is possible that the ORP signal is buffered to high values by the presence/formation of such oxidized species despite the absence of O_2, and that until the probe meets important dissolved reduced species. Second, in lakes Alchichica, La Preciosa and Alberca, we see the decrease of ORP is more closely associated with the end of Chl a and/or phycocyanin peaks. This suggests that there may be a local production of dissolved oxygen still, but it is quickly consumed (e.g. through respiration) and is thus not measured. Yet it would act as a buffer for the ORP signal until Chl a and/or phycocyanin disappear.

II. Calculation of equilibrium isotopic fractionation between DIC and solid carbonates

Carbonate precipitation is associated with a temperature- and mineralogy-dependent isotopic fractionation such that bottom sediment carbonates indirectly record the lake DIC isotopic composition following:

$$\delta^{13}C_{carb} = \delta^{13}C_{DIC} + \Delta^{13}C_{carb\text{-}DIC}(\text{Temp., R-}CO_3)$$

where $\Delta^{13}C_{carb\text{-}DIC}$ is the isotopic fractionation between DIC and carbonate ('R-CO_3' designating the influence of different carbonate mineralogy). Thus, calculating the initial isotopic composition of the DIC from which a bulk carbonate assemblage has precipitated from requires to know the proportion of the different carbonate phases. More precisely, we consider the isotopic fractionation with the carbonate ions ($CO_3^{2-}{}_{(aq)}$) from which the carbonate minerals actually precipitate. A weighted average fractionation can be calculated such as:

$$\Delta_{bulk\_carbonate\text{-}CO3} = \Sigma\, \Delta_{i\_carb\text{-}CO3} * f_i$$

where f_i is the proportion of each carbonate phase and $\Delta_{i\_carb\text{-}CO3}$ the isotopic fractionation between each of these and the $CO_3^{2-}{}_{(aq)}$. The sediments mineralogical assemblages were determined by XRD (see main text for method). In the four Mexican lake sediments, the carbonate mix is composed of aragonite mainly, with minor calcite and/or hydromagnesite. Considering an annual average temperature of 16 °C, the isotopic fractionation ($\Delta_{i\_carb\text{-}CO3}$) linked to the precipitation of these phases equals to 1.0, -0.8 and 3.5 ‰, respectively. References for the equations used in the calculations are shown in Table S5.

Looking at the first most recent layer of sediments in each lake, we find the isotopic composition of the DIC in equilibrium with the carbonates ($\delta^{13}C_{CO3\text{-}eq}$) to be 3.1, 1.7, 1.7 and -0.8 ‰ in lakes Alchichica, Atexcac, La Preciosa

and Alberca, respectively (Table S5). This $\delta^{13}C_{CO3\text{-}eq}$ can then be compared with $\delta^{13}C_{CO3}$ of the lakes water column, whose method of calculation can be found below in the supplementary part II. In lakes Alchichica, La Preciosa and Alberca, $\delta^{13}C_{CO3\text{-}eq}$ corresponds to a $\delta^{13}C_{CO3}$ value of the water column and more precisely, to the top of their oxycline/thermocline, i.e. before oxygen and temperature start to decrease (Tables S4 and S5). In lake Atexcac, $\delta^{13}C_{CO3\text{-}eq}$ is, within uncertainty, in equilibrium with $\delta^{13}C_{CO3}$. This could be due to some detrital contributions from microbialites with lower $\delta^{13}C$ covering parts of the crater's walls (Fig. S1) to the sediments.

III. Calculation of $\delta^{13}C$ signatures from the different DIC species ($CO_{2(aq)}$, HCO_3^-, CO_3^{2-}) from the bulk $\delta^{13}C_{DIC}$

The analytical method for DIC isotopes quantification allows to measure the bulk DIC isotopic composition (see method in the main text), integrating the weighted average of $CO_{2(aq)}$, HCO_3^- and CO_3^{2-} respective isotopic compositions such as:

$$\delta^{13}C_{DIC} = ([HCO_3]*\delta^{13}C_{HCO3} + [CO_3]*\delta^{13}C_{CO3} + [CO_2]*\delta^{13}C_{CO2}) / [DIC] , \quad (1)$$

However, strong isotopic fractionations of about 10 ‰ exist between the dissolved $CO_{2(aq)}$ and the two other DIC species (e.g. Mook et al., 1974). At the pH of the studied Mexican lakes (~ 9), $CO_{2(aq)}$ represents less than 0.5 % of total DIC (Table S4). Therefore, its isotopic composition significantly differs from that of the bulk DIC and needs to be calculated *a posteriori* when considering processes involving CO_2 specifically.

We can isolate and calculate $\delta^{13}C_{CO2}$ by using the isotopic fractionation between the different DIC species ($\alpha_{X\text{-}Y}$). The "per mil fractionation" $1000ln\alpha_{X\text{-}Y}$ – when around 10 ‰ or less – is almost identical to the isotopic difference between different species ($\Delta^{13}C_{X\text{-}Y} = \delta^{13}C_X - \delta^{13}C_Y$) (Sharp, 2017). Therefore, we use $\Delta^{13}C$ to derive Eq. (1) such as:

$$\delta^{13}C_{CO2} = \delta^{13}C_{DIC} - ([HCO_3]*\Delta^{13}C_{HCO3\text{-}CO2} - [CO_3]*\Delta^{13}C_{CO3\text{-}CO2}) / [DIC], \quad (2)$$

We used $\Delta^{13}C$ data from Emrich et al. (1970) who provide isotopic fractionations between all three DIC species as a function of temperature. All temperatures and resulting isotopic fractionations and compositions are summarized in Table S5.

IV. Chlorophyll a peak in the hypolimnion of Alberca de los Espinos

In Alberca de los Espinos we recorded a peak of purported chlorophyll a (Chl. a) in the anoxic waters between 15 and 20 m in depth, reaching the same concentrations as in the upper oxygenated waters (Fig. 2). However, this photosynthetic pigment is used as a proxy for oxygenic photosynthesis and thus not usually found in anoxic conditions.

The occurrence of oxygenic organisms in anoxic waters could have several explanations: (i) the Chl. a peak corresponds to a daily vertical migration of phytoplankton, (ii) the distribution of planktonic ecological niches with depth is inherited from the mixing period and did not change despite seasonally implemented stratification of the water column at the time of sampling or (iii) the Chl. a detected by the multi-parameter probe is mistaken with

another photosynthetic pigment, such as the bacteriochlorophyll of anaerobic microorganisms which have similar absorption and emission spectra (Taniguchi and Lindsey, 2021 and references therein).

The first two possibilities rely on the presence of cyanobacteria and/or eukaryotic algae under anoxic conditions either as "dormant" forms or active forms with a facultative anaerobic activity. A significant [DOC] increase at the same depth as this Chl. a peak suggests the presence of active organisms releasing DOC in the anoxic waters (~17 m, Fig. 3). Meanwhile, cyanobacteria can be specifically targeted by the phycocyannin pigment and are only found to match the Chl. a peak around 12-13 m (Fig. 2). Besides, unicellular eukaryotic algae do not perform anoxygenic photosynthesis (Atteia et al., 2013). Alternatively, aerobic unicellular photosynthetic eukaryotes forced to anoxic conditions can switch to fermentative metabolism (Atteia et al., 2013) which could participate to the DOC production observed at 17 m depth (Fig. 3). However, their presence in the anoxic waters despite more favorable conditions in shallower oxygenated waters of the lake where green algae thrive (Chl. a peak between 5 and 10 m, Fig. 2) seems unlikely.

Moreover, anoxic waters of stratified water bodies are typical habitats of anoxygenic photosynthesizers such as green or purple sulfur bacteria (GSB and PSB, respectively) (e.g. Fulton et al., 2018). These organisms usually operate under deeper and darker conditions than oxygenic organisms and use photosynthetic pigments different than Chl. a. Namely, GSB synthetize bacteriochlorophyll (BChl.) c, d or e while PSB synthesize BChl. a as their main photosynthetic pigments (Fulton et al., 2018; Hamilton, 2019). Although the molecular composition of these pigments slightly differs from one another, some of them share close optical characteristics with Chl. a. Notably, BChl. c and d and Chl. a share B and Q bands of absorption at around 430 and 660 nm, respectively (see Table 1 in Taniguchi and Lindsey, 2021). Meanwhile BChl. a bands are very distant from these values (~ 360 and 770 nm). Furthermore, BChl c, d and e and Chl. a also share very close fluorescence wavelengths around 670 nm while BChl. a reemits around 790 nm (Table 2 in Taniguchi and Lindsey, 2021). Since the multi-parameter probe that we used detects Chl. a based on these absorption and reemission wavelengths, it would likely confuse Chl. a with BChl. c and d (and possibly BChl. e) which are characteristic pigments of GSB. However, it should differentiate Chl. a and BChl. a (characteristic of PSB).

In conclusion, the third chlorophyll a peak in the anoxic waters of Lake Alberca could partly be the result of vertical migration of oxygenic photosynthetic organisms, but it more likely represents a bias of the probe towards bacteriochlorophylls pigments typical of green sulfur bacteria, reflecting the presence and activity of anoxygenic phototrophs at these depths.

V. Calculation of the methane $\delta^{13}C$ endmember from the sediment porewaters of Lake Alberca de los Espinos

In Alberca de los Espinos, the isotopic composition of DIC strikingly increases from the middle of the lake water column to the first 10 cm of sediment porewaters (Table 2 and S4). This can be well explained by the action of acetoclastic methanogenesis which degrades sedimentary OM to produce ^{13}C-depleted methane and ^{13}C-rich carbon dioxide diffusing upward in the water column (main text part 5.2.4). Following the simplified equation

$$CH_3COOH \rightarrow CO_2 + CH_4 , \qquad (3)$$

the C isotopic composition of methane ($\delta^{13}C_{CH4}$) can be calculated by mass balance based on C isotopic compositions of sedimentary OC and dissolved CO_2 ($\delta^{13}C_{SOC}$ and $\delta^{13}C_{CO2}$, respectively) such that:

$$\delta^{13}C_{SOC} = 0.5*\delta^{13}C_{CO2} + 0.5*\delta^{13}C_{CH4}\ , \qquad (4)$$

and thus:

$$\delta^{13}C_{CH4} = 2*\delta^{13}C_{SOC} - \delta^{13}C_{CO2}\ . \qquad (5)$$

Following Eq. (5), we calculate $\delta^{13}C_{CH4}$ at depth where $\delta^{13}C_{SOC}$ and $\delta^{13}C_{CO2}$ are available, *i.e.* at 0.5 and 7 cm depths within the sediments of Lake Alberca (Table S4).

In this calculation, we consider that the isotopic composition of the sedimentary organic carbon that we measured corresponds to the one used by methanogen organisms. Moreover, we consider that the bulk isotopic composition of porewater DIC ($\delta^{13}C_{DIC}$) is related to methanogenesis. This is supported by the fact that (i) the very positive $\delta^{13}C_{DIC}$ can unequivocally be explained by methanogenesis while differing from the water column $\delta^{13}C_{DIC}$ and (ii) that the DIC concentration gradient between the porewater and the lake water forces the DIC to diffuse from the porewater to the lake water rather than the other way around. Nonetheless, we consider that there is isotopic exchange between the different DIC species of the porewater and lake water (as suggested by the diffusion of DIC through the porewaters and sediment-water interface). Hence, we use the calculated $\delta^{13}C_{CO2}$ value rather than bulk $\delta^{13}C_{DIC}$ in the calculation of Eq. (5).

Numerical derivation of Eq. (5) for depths 0.5 and 7 cm in the sediments are $\delta^{13}C_{CH4}$ = -59.0 ‰ and $\delta^{13}C_{CH4}$ = -57 ‰, respectively.

Supplementary Figures

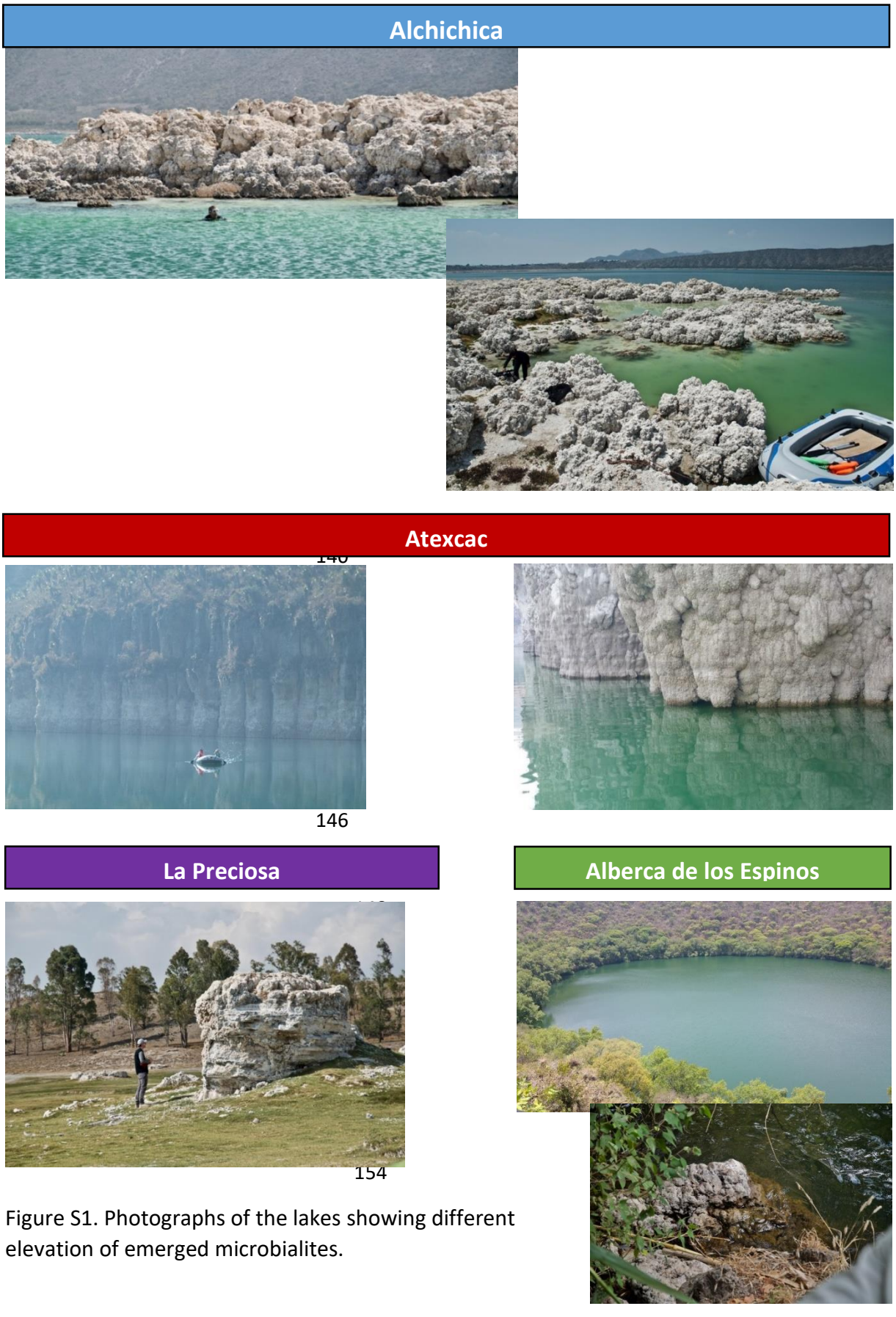

Figure S1. Photographs of the lakes showing different elevation of emerged microbialites.

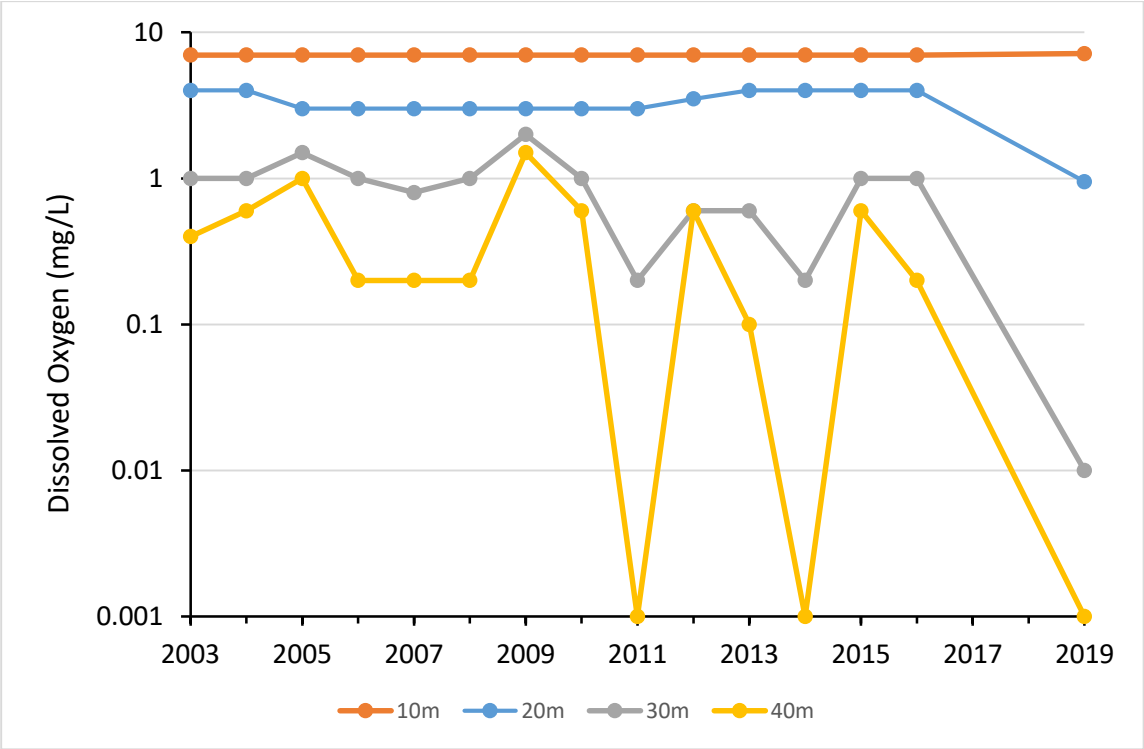

Figure S2. Dissolved oxygen (DO) concentrations in mg/L at 10, 20, 30 and 40m depth in lake Alchichica in May since 2003. Data between 2003 and 2017 from Macek et al., 2020. We notice that DO is lower in 2019 than other years at each depth pointing out the sharper stratification of the lake in 2019.

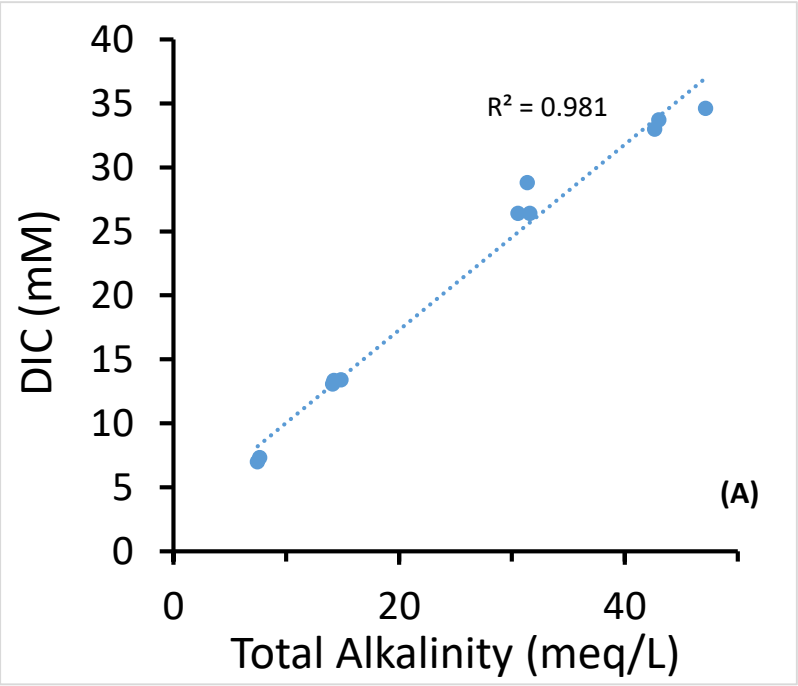

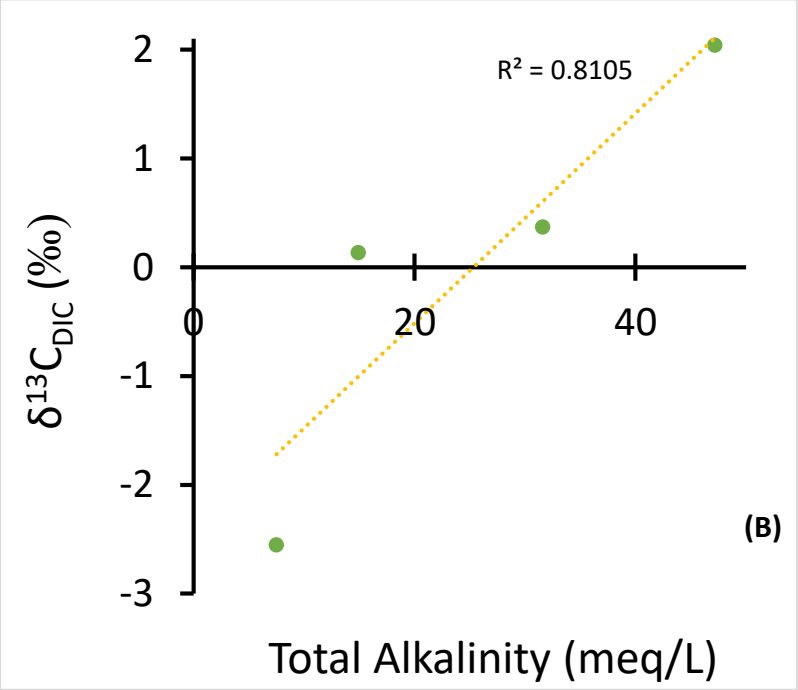

Figure S3:

Correlation between the total alkalinity of the four lakes in meq/L and their DIC concentration (A) and isotopic composition (B). Data from 2019 (this study) and 2012/2014 (Zeyen et al., 2021) are plotted in (A).

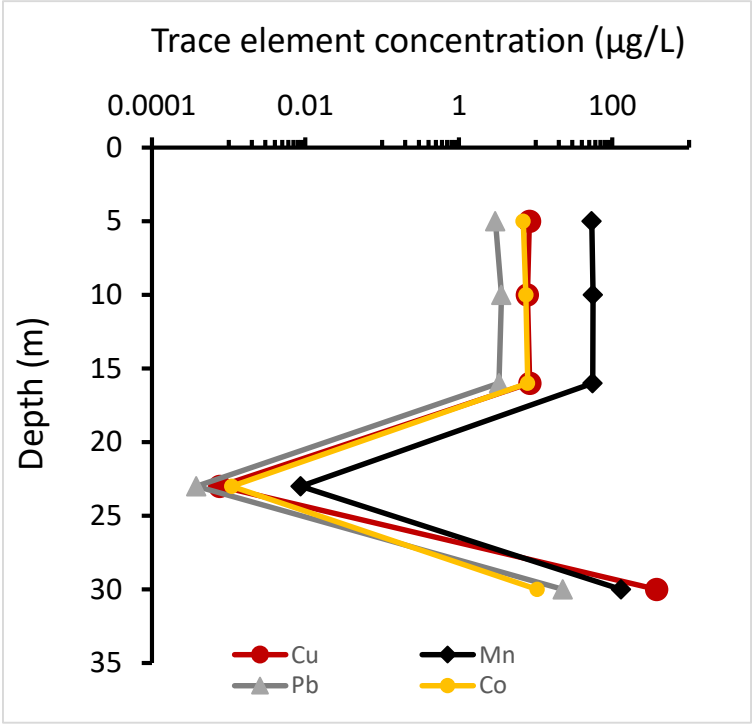

Figure S4. Depth profile of several metal ions dissolved in the waters of Lake Atexcac.

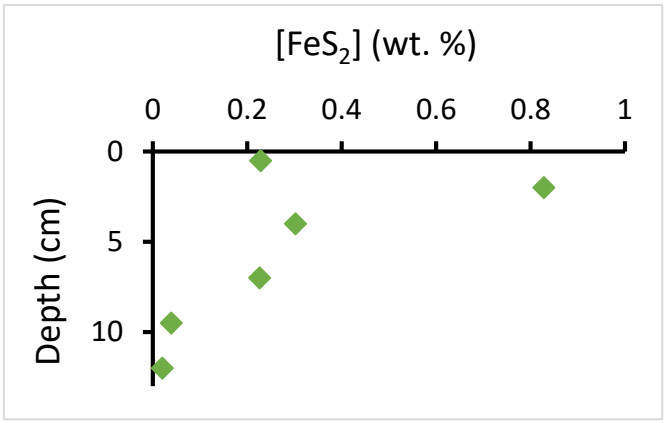

Figure S5. Pyrite concentrations in weight percent in the surficial sediments of Lake Alberca de los Espinos.

Supplementary Tables

Table S1

Concentrations and isotopic compositions of dissolved inorganic carbon (DIC) and particulate organic carbon (POC) and C:N molar ratios of particulate organic matter (POM).

Lake	Sample	DIC	POC	$(C:N)_{POM}$	$\delta^{13}C_{DIC}$	$\delta^{13}C_{POC}$
		mmol/L		(molar)	‰	
Alchichica	AL 5m	35.0	0.07	10.6	2.0	-26.7
	AL 10m	33.0			2.0	
	AL 20m	34.6			1.6	
	AL 30m	34.6	0.10	10.5	1.7	-26.3
	AL 35m	34.9	0.02	8.1	1.6	-25.7
	AL 40m	34.7	0.02	7.1	1.6	-25.1
	AL 50m	34.8			1.6	
	AL 55m	34.8	0.01	5.9	1.5	-24.1
	AL 58m	34.8			1.6	
	AL 60m	34.6			1.5	
Atexcac	ATX 5m	26.4	0.05	9.3	0.4	-28.4
	ATX 10m	26.2	0.05	9.8	0.4	-28.2
	ATX 16m	26.8	0.05	9.8	0.3	-29.0
	ATX 23m	24.2	0.02	6.5	0.9	-26.7
	ATX 30m	25.7	0.02	6.6	0.2	-26.4
La Preciosa	LP 5m	13.4	0.06	11.6	0.1	-26.4
	LP 8m		0.07	10.4		-27.1
	LP 10m	13.4	0.06	12.2	0.2	-27.4
	LP 12.5m	11.5	0.06	10.5	-0.2	-27.1
	LP 15m	13.4	0.03	8.2	-0.3	-23.5
	LP 20m	13.3	0.02	7.4	-0.4	-26.3
	LP 31m	13.3	0.02	7.3	-0.4	-25.2
Alberca de Los Espinos	Albesp 5m	6.8	0.04	8.5	-2.6	-27.0
	Albesp 7m	7.1	0.03	8.3	-2.3	-26.2
	Albesp 10m	7.2	0.02	7.5	-4.1	-28.3
	Albesp 17m	7.2	0.05	6.7	-3.4	-29.0
	Albesp 20m	7.9	0.05	6.3	-3.3	-26.5
	Albesp 25m	8.7	0.06	6.5	-2.0	-25.7

Table S2

Calculated activities of the different dissolved inorganic carbon species, CO_2 partial pressure (P_{CO2}), ratio of P_{CO2} with atmospheric P_{CO2} at 2320m altitude and pH presented for waters at different depths in 2019 and surface waters of years 2012 and 2014 (calculated with data from Zeyen et al., 2019).

Lake	Sample	$a(CO_{2(aq)})$	$a(HCO_3^-)$	$a(CO_3^{2-})$	PCO_2	PCO_2 / $PCO_{2\text{-atm}}$	pH
			LOG10		LOG10 (atm)		
Alchichica	**AL 5m**	-4.48	-1.73	-2.98	-3.01	3.2	9.14
	AL 10m	-4.60	-1.77	-2.94	-3.13	2.4	9.22
	AL 20m	-4.56	-1.74	-2.93	-3.09	2.7	9.23
	AL 30m	-4.54	-1.74	-2.94	-3.07	2.8	9.22
	AL 40m	-4.56	-1.74	-2.92	-3.09	2.7	9.24
	AL 50m	-4.47	-1.72	-2.98	-3.00	3.3	9.17
	AL 55m	-4.48	-1.72	-2.97	-3.01	3.2	9.18
	AL 60m	-4.57	-1.74	-2.92	-3.10	2.6	9.25
Atexcac	**ATX 5m**	-4.30	-1.83	-3.35	-2.83	4.9	8.85
	ATX 10m	-4.29	-1.83	-3.36	-2.82	4.9	8.85
	ATX 16m	-4.26	-1.81	-3.37	-2.79	5.3	8.85
	ATX 23m	-4.25	-1.85	-3.45	-2.78	5.4	8.82
	ATX 30m	-4.23	-1.82	-3.43	-2.76	5.7	8.82
La Preciosa	**LP 5m**	-4.67	-2.04	-3.40	-3.20	2.1	9.02
	LP 8m	-4.65	-2.03	-3.41	-3.18	2.2	9.01
	LP 10m	-4.60	-2.03	-3.45	-3.13	2.4	8.97
	LP 12.5m	-4.60	-2.08	-3.57	-3.13	2.4	8.92
	LP 15m	-4.48	-2.01	-3.55	-3.01	3.2	8.88
	LP 20m	-4.48	-2.01	-3.56	-3.01	3.2	8.88
	LP 31m	-4.48	-2.01	-3.56	-3.01	3.2	8.88
Alberca de Los Espinos	**Albesp 5m**	-5.05	-2.30	-3.53	-3.58	0.9	9.12
	Albesp 7m	-5.00	-2.27	-3.54	-3.53	1.0	9.09
	Albesp 10m	-4.58	-2.23	-3.88	-3.11	2.6	8.73
	Albesp 17m	-4.53	-2.23	-3.93	-3.06	2.9	8.7
	Albesp 20m	-3.88	-2.18	-4.47	-2.41	12.7	8.11
	Albesp 25m	-3.40	-2.14	-4.89	-1.93	38.7	7.66
	Surface						
Alchichica	janv-12	-4.40	-1.74	-3.08	-2.93	3.9	9.08
	mai-14	-4.36	-1.72	-3.08	-2.89	4.3	9.02
Atexcac	janv-12	-4.14	-1.80	-3.47	-2.67	7.0	8.75
	mai-14	-3.81	-1.74	-3.66	-2.34	15.2	8.45
Alberca	mai-14	-4.54	-2.23	-3.91	-3.07	2.8	8.67
La Preciosa	janv-12	-4.50	-2.03	-3.56	-3.03	3.1	8.88
	mai-14	-4.37	-2.01	-3.64	-2.90	4.1	8.75

200 Table S3

201 Analyses of surficial solid sediments and porewaters: sedimentary organic matter C:N ratio; concentrations and
202 isotopic compositions of sedimentary organic carbon (SOC); concentrations and isotopic compositions of DIC in
203 the porewaters and solid bulk carbonates.

Lake	**Sample name**	**Depth**	**$(C:N)_{SOM}$**	**SOC**	**$\delta^{13}C_{SOC}$**	**DIC**	**$\delta^{13}C_{DIC}$**	**Carb.**	**$\delta^{13}C_{Carb}$**
		cm	(molar)	wt. %	‰	mmol/L	‰	wt. %	‰
Alchichica	AL19_C2a_01	0-1	10.4	5.1	-25.7	35.8	0.4	41	4.6
	AL19_C2a_02	1-3	10.2	4.7	-25.7	36.2	0.0	44	4.5
	AL19_C2a_03	3-5	10.6	4.3	-25.3	36.8	-0.1	ND.	4.5
	AL19_C2a_04	5-7	10.4	3.8	-25.1	34.5	-0.3	40	4.7
	AL19_C2a_05	7-10	10.4	3.8	-24.6	34.6	-0.4	35	4.5
	AL19_C2a_06	10-13	10.4	3.7	-24.5	34.9	-0.5	38	4.8
Atexcac	ATX19_C1_1	0-1	8.2	0.9	-26.7	24.4	0.3	61	2.5
	ATX19_C1_2	1-2	7.9	1.3	-26.8	22.5	-0.2	46	2.7
	ATX19_C1_3	2-4	8.0	1.1	-26.8	20.7	0.4	61	2.7
	ATX19_C1_S4	4-7	8.6	0.9	-27.0	ND.	ND.	71	2.5
	ATX19_C1_4	7-9	8.7	0.9	-26.8	22.7	0.5	ND.	2.1
	ATX19_C1_5	9-10	9.3	1.0	-26.9	23.1	0.5	64	2.1
	ATX19_C1_S6	10-12	9.6	0.8	-27.0	25.7	0.0	69	2.1
La Preciosa	LP16_C3_7	0-2	9.8	2.3	-25.1	ND.	ND.	61	2.6
	LP16_C3_8	2-4	9.6	2.3	-25.8	ND.	ND.	63	2.6
	LP16_C3_9	8-10	11.0	2.6	-23.2	ND.	ND.	54	2.5
Alberca de Los Espinos	ALBESP19_C3_1	0-1	13.1	13.3	-28.6	11.2	9.4	20	-1.5
	ALBESP19_C3_2	1-3	12.3	19.0	-29.4	ND.	ND.	18	ND.
	ALBESP19_C3_3	3-5	11.8	16.2	-29.2	ND.	ND.	17	ND.
	ALBESP19_C3_4	5-9	11.6	11.9	-27.9	11.9	7.7	15	-1.5
	ALBESP19_C3_S5	9-10	14.3	7.5	-25.7	ND.	ND.	12	ND.
	ALBESP19_C3_5	10-14	13.5	5.5	-25.4	ND.	ND.	12	ND.

204

205

Table S4

Ionic concentrations in the water columns of the four lakes. TDS stands for 'total dissolved S', and was measured by ICP-AES. Fe and Mn were measured by ICP-MS. The Cl^- and SO_4^{2-} by chromatography.

Lake	Sample	TDP	NH4+	Fe	Mn	SO_4^{2-}	TDS	Cl-
		µmoles/L				mmoles/L		
Alchichica	AL 4.9m	0.3	3.1	0.3	1.4	11.82	10.15	107
	AL 5m	0.4	2.9	0.2	1.5	11.86	10.25	107
	AL 10m	0.4	2.4	0.3	1.7	11.79	10.13	106
	AL 20m	0.5	3.5	0.2	0.4	11.76	10.05	106
	AL 30m	1.6	2.9	0.2	0.4	11.70	10.12	106
	AL 40m	1.8	3.5	0.1	0.5	11.81	9.97	107
	AL 50m	2.5	3.3	<LD	0.4	12.01	10.02	108
	AL 55m	2.6	13.0	<LD	0.5	12.03	9.70	109
	AL 60m	3.2	3.9	0.1	1.0	12.24	10.02	111
Atexcac	ATX 5m	0.3	2.4	0.8	1.0	2.51	2.45	122
	ATX 10m	0.2	2.4	0.7	1.0	2.53	2.42	122
	ATX 16m	0.2	2.5	0.4	1.0	2.48	2.45	121
	ATX 23m	0.4	2.5	0.2	0.0	2.64	2.46	126
	ATX 30m	0.5	2.9	0.1	2.4	2.53	2.45	124
La Preciosa	LP 5m	0.2	1.8	0.1	1.1	1.22	1.20	8.4
	LP 8m	0.2	2.0	<LD	0.3	1.20	1.21	8.2
	LP 10m	0.2	1.6	<LD	0.4	1.17	1.19	8.0
	LP 12.5m	0.2	1.4	<LD	0.4	1.15	1.19	7.8
	LP 15m	<LD	2.0	<LD	0.6	1.16	1.20	7.9
	LP 20m	0.3	2.3	<LD	1.4	1.16	1.18	7.9
	LP 30m	0.3	2.2	<LD	1.0	1.16	1.20	7.9
Alberca de Los Espinos	Albesp 5m	2.9	2.4	<LD	1.5	0.01	0.009	4.2
	Albesp 7m	3.0	3.1	<LD	0.8	<LD	0.008	4.2
	Albesp 10m	7.6	3.5	<LD	0.5	<LD	0.006	4.0
	Albesp 17m	11.0	2.5	<LD	0.6	<LD	0.009	4.0
	Albesp 20m	15.6	8.5	<LD	1.0	<LD	0.008	4.2
	Albesp 25m	27.4	3.3	0.2	1.9	<LD	0.013	4.2

220 Table S5

221 Iron, sulfur and manganese concentrations in the particulate matter, measured with ICP-AES. <LD =
222 below detection limits.

Lake	Sample	Fe	S	Mn
		10^3*µmoles/L		
Alchichica	AL 4.9m	178	3426	7
	AL 30m	61	1224	3
	AL 35.6m	64	1631	<LD
	AL 40.6m	47	1630	0.2
Atexcac	ATX 5m	821	1624	15
	ATX 10m	973	2486	21
	ATX 16m	368	1195	20
La Preciosa	LP 5m	295	553	70
	LP 8m	236	575	52
	LP 10m	305	525	76
	LP 12.5m	390	661	108
	LP 15m	194	452	124
Alberca de Los Espinos	Albesp 5m	25	57	29
	Albesp 7m	26	50	28
	Albesp 10m	20	68	63
	Albesp 17m	24	97	1173
	Albesp 20m	230	90	996
	Albesp 25m	5974	561	156

223

Table S6

Isotopic fractionations between the different DIC species according to the temperature at different depths in the water columns; calculated based on fractionation equations by Emrich et al., 1970. The $\delta^{13}C_{DIC}$ of sample 'LP 8m' was not measured, thus the corresponding $\delta^{13}C_{CO2(aq)}$ and $\delta^{13}C_{CO3^{2-}(aq)}$ were calculated based on the average $\delta^{13}C_{DIC}$ of samples beneath and below.

Lake	Sample	Temperature	$\Delta^{13}C_{HCO3\text{-}CO2(aq)}$	$\Delta^{13}C_{CO3\text{-}CO2(aq)}$	$\delta^{13}C_{CO2(aq)}$	$\delta^{13}C_{CO32\text{-}(aq)}$
		°C		‰		
Alchichica	**AL 5m**	19.2	9.7	11.5	-7.7	3.5
	AL 10m	18.9	9.7	11.6	-7.8	3.4
	AL 20m	16.3	10.0	12.0	-8.5	3.1
	AL 30m	15.5	10.1	12.1	-8.5	3.2
	AL 40m	15.3	10.1	12.1	-8.7	3.1
	AL 50m	15.2	10.1	12.1	-8.6	3.1
	AL 55m	15.2	10.1	12.1	-8.7	3.1
	AL 60m	15.2	10.1	12.1	-8.7	3.0
Atexcac	**ATX 5m**	20.1	9.5	11.4	-9.2	1.9
	ATX 10m	19.7	9.6	11.4	-9.1	1.9
	ATX 16m	17.2	9.9	11.8	-9.5	2.0
	ATX 23m	15.7	10.1	12.1	-9.1	2.6
	ATX 30m	15.6	10.1	12.1	-9.8	1.9
La Preciosa	**LP 5m**	19.5	9.6	11.5	-9.5	1.7
	LP 8m	19.0	9.7	11.6	-9.5	1.8
	LP 10m	18.3	9.8	11.7	-9.5	1.8
	LP 12.5m	17.0	9.9	11.9	-10.0	1.6
	LP 15m	16.2	10.0	12.0	-10.3	1.4
	LP 20m	15.6	10.1	12.1	-10.4	1.4
	LP 31m	15.4	10.1	12.1	-10.4	1.4
Alberca de Los Espinos	**Albesp 5m**	22.8	9.2	11.0	-11.8	-1.1
	Albesp 7m	22.1	9.3	11.1	-11.7	-0.8
	Albesp 10m	19.6	9.6	11.5	-13.6	-2.3
	Albesp 17m	17.4	9.9	11.8	-13.1	-1.5
	Albesp 20m	16.9	9.9	11.9	-12.9	-1.2
	Albesp 25m	16.7	9.9	11.9	-11.3	0.5

Table S7

Carbonates mineralogical and isotopic data from the first layer of sediments in the four Mexican lakes. Bulk carbonate concentrations were determined by acid decarbonatation. Relative concentrations of carbonate phases normalized by the total carbonate content were determined after XRD and Rietveld refinement analyses. Calculations of C isotope fractionation ($\Delta^{13}C_{Carb\text{-}CO3}$) at 16 °C for aragonite and calcite are based on equations from Romanek et al. (1992) and Emrich et al. (1970) and those for hydromagnesite on Aharon (1988) (equivalent to Harrison et al., 2021) and Emrich et al. (1970).

Sample name	**Depth**	**Carb.**	**$\delta^{13}C_{Carb}$**	**Relative proportion of each carbonate phase to the total carbonate content (in %)**			**$\Delta^{13}C_{Carb\text{-}CO3}$**	**$\delta^{13}C_{CO3\text{-}eq}$**
	cm	wt. %	‰	Aragonite	Calcite	Hydromagnesite	‰	‰
AL19_C2a_01	0-1	41	4.6	72	4	23	1.5	3.1
ATX19_C1_1	0-1	61	2.5	92	8	0	0.9	1.7
LP16_C3_7	0-2	61	2.6	96.5	3.5	0	0.9	1.7
ALBESP19_C3_1	0-1	20	-1.6	0	100	0	-0.8	-0.8

References

Aharon, P.: A stable-isotope study of magnesites from the Rum jungle uranium field, Australia: implications for the origin of strata-bound massive magnesites. Chemical Geology, 69, 127-145. https://doi.org/10.1016/0009-2541(88)90164-7 , 1988.

Atteia, A., van Lis, R., Tielens, A.G. and Martin, W.F.: Anaerobic energy metabolism in unicellular photosynthetic eukaryotes. (BBA)-Bioenergetics, 1827, 210-223. https://doi.org/10.1016/j.bbabio.2012.08.002 , 2013.

Bade, D.L., Carpenter, S.R., Cole, J.J., Hanson, P.C., Hesslein, R.H.: Controls of δ^{13}C-DIC in lakes: Geochemistry, lake metabolism, and morphometry. Limnol. Oceanogr. 49, 1160–1172. https://doi.org/10.4319/lo.2004.49.4.1160 , 2004.

Emrich, K., Ehhalt, D.H., Vogel, J.C.: Carbon isotope fractionation during the precipitation of calcium carbonate. Earth Planet. Sci. Lett. 8, 363–371. https://doi.org/10.1016/0012-821X(70)90109-3 , 1970.

Fulton, J.M., Arthur, M.A., Thomas, B., Freeman, K.H.: Pigment carbon and nitrogen isotopic signatures in euxinic basins. Geobiology 16, 429–445. https://doi.org/10.1111/gbi.12285 , 2018.

Hamilton, T.L.: The trouble with oxygen: The ecophysiology of extant phototrophs and implications for the evolution of oxygenic photosynthesis. Free Radical Biology and Medicine, 140, 233-249. https://doi.org/10.1016/j.freeradbiomed.2019.05.003 , 2019.

Harrison, A.L. Bénézeth, P., Schott, J., Oelkers, E.H., Mavromatis, V.: Magnesium and carbon isotope fractionation during hydrated Mg-carbonate mineral phase transformations, Geochimica et Cosmochimica Acta, 293, 507-524. https://doi.org/10.1016/j.gca.2020.10.028 , 2021,

Macek, M., Medina, X.S., Picazo, A., Peštová, D., Reyes, F.B., Hernández, J.R.M., Alcocer, J., Ibarra, M.M., Camacho, A.: Spirostomum teres: A Long Term Study of an Anoxic-Hypolimnion Population Feeding upon Photosynthesizing Microorganisms. Acta Protozool. 59, 13–38. https://doi.org/10.4467/16890027AP.20.002.12158 , 2020.

Mook, W.G., Bommerson, J.C., Staverman, W.H.: Carbon isotope fractionation between dissolved bicarbonate and gaseous carbon dioxide. Earth Planet. Sci. Lett. 22, 169–176. https://doi.org/10.1016/0012-821X(74)90078-8 , 1974.

Romanek, C.S., Grossman, E.L., Morse J.W.: Carbon isotopic fractionation in synthetic aragonite and calcite: Effects of temperature and precipitation rate. Geochimica et Cosmochimica Acta, 56, 419-430, https://doi.org/10.1016/0016-7037(92)90142-6 , 1992.

Sharp, Z.: Principles of stable isotope geochemistry. https://doi.org/10.25844/h9q1-0p82 , 2017.

Taniguchi, M. and Lindsey, J.S.: Absorption and fluorescence spectral database of chlorophylls and analogues. Photochemistry and Photobiology, 97, 136-165. https://doi.org/10.1111/php.13319 , 2021.